ACS Catalysis

Review

pubs.acs.org/acscatalysis

What Makes a Good Catalyst for the Deacon Process?

Herbert Over*,† and Reinhard Schomäcker*,‡

†Physikalisch-Chemisches Institut, Justus-Liebig-Universität Gießen, Heinrich-Buff-Ring 58, D-35392 Gießen, Germany

‡Department of Chemistry, Technical University Berlin, D-10623 Berlin, Germany

ABSTRACT: The Deacon process is a sustainable way to recover chlorine from HCl by its oxidation with molecular oxygen. Deacon catalysts need to fulfill both selection criteria: high activity and high stability. In this Review, we introduce and discuss simple descriptors for assessing activity and stability of catalyst materials. A promising descriptor for ranking the experimental activities of Deacon catalysts and other oxidation catalysts in the form of oxides represents the dissociation energy of molecular oxygen as introduced by Studt et al. (*ChemCatChem.* **2010**, *2*, 98). The resulting volcano plot allows for identifying promising catalyst materials for the Deacon process, such as exemplified with La_2O_3.

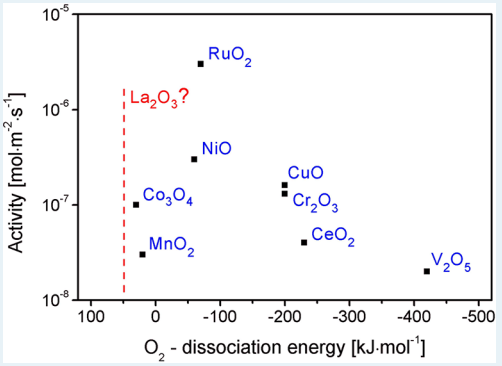

KEYWORDS: *Deacon process, volcano curve, BEP relation, HCl oxidation, heterogeneous catalysis, stability, activity*

1. INTRODUCTION

The oxidation of HCl by molecular oxygen to form H_2O and Cl_2 is a sustainable way to recover molecular chlorine from HCl waste. Since oxidation of HCl is far too slow to proceed in the homogeneous gas phase below 800 K, efficient catalysts have to be employed (Deacon process).[1−3] However, there are two fundamental problems encountered with Deacon catalysts. These are the lack of stability under such harsh reaction conditions and insufficient activity.

The Deacon process was introduced some 150 years ago by Henry Deacon.[4] The original Deacon catalyst is based on $CuO/CuCl_2$ but has suffered most notably from low stability as a result of formation of volatile copper chloride species and too low activity so that the needed reaction temperature is above 400 °C. The HCl oxidation reaction is only slightly exothermic, by −59 kJ/mol per mol Cl_2, and therefore, the HCl equilibrium conversion is significantly reduced at reaction temperatures above 350 °C. Over the past century, several alternative Deacon catalysts have been proposed,[5−13] but most of them were either not stable or not active enough so that electrolysis has been the industrially applied method of choice to recover Cl_2 from HCl waste.[14]

Only recently, in 1999, Sumitomo Chemical developed a new type of Deacon catalyst that is based on RuO_2 coated on rutile TiO_2.[1] The main advantage of this catalyst is that RuO_2 is highly active in the oxidation of HCl so that the reaction temperature can be reduced to about 300 °C, where the RuO_2−based catalyst is quite stable. Around 300 °C, in-depth chlorination is suppressed because of selective and self-limiting surface chlorination.[15−18]

Among the potential catalysts for the Deacon process, the activity in the HCl oxidation reaction varies widely.[2,19] Therefore, we asked ourselves whether there are simple indicators or descriptors available that allow us to rank the relative activities of catalysts in the Deacon process. The original Deacon process over $CuO/CuCl_2$ was shown to consist of two consecutive solid state reactions of the catalyst, namely, the chlorination of the oxidic catalyst and reoxidation of the chlorinated catalyst,[19,20] during which the desired product Cl_2 is released. A first approach to rank the activity of Deacon catalysts goes back to Allen,[20] who recognized that an active Deacon catalyst is correlated with a material for which the endothermic reoxidation step of the chlorinated surface/material is not too demanding.

Recently, Studt et al.[21,22] have systematically studied the HCl oxidation reaction on various rutile oxide surfaces (TiO_2, IrO_2, RuO_2, and other rutile oxides) using density functional theory (DFT) calculations. They found that the dissociation energy of molecular oxygen is a proper descriptor to assess the activity of oxide surfaces in the Deacon process. A simple descriptor should be based on a thermodynamic parameter rather than on a full kinetic analysis to be feasible and well accessible. Also in this Review, we shall follow this approach by relating experimental activity data of the catalyzed HCl oxidation to the descriptor proposed by Studt et al.[21] in terms of the O_2 dissociation energy (Section 2), thus establishing a volcano-type dependence of the activity data among the various Deacon catalysts.

Another issue that we want to address in this Review is the stability of the Deacon catalyst. For industrial application, the long-term stability is actually even more important than very high activity. Again, we ask ourselves whether there are

Received: November 14, 2012
Revised: March 20, 2013
Published: April 4, 2013

   dx.doi.org/10.1021/cs300735e | *ACS Catal.* 2013, 3, 1034−1046

thermodynamically based indicators/descriptors that allow us to predict the stability of a catalyst under HCl oxidation reaction conditions. If in-depth chlorination of catalysts and the formation of volatile chloride species are considered to be the main reasons for the instability of a Deacon catalyst, then the thermodynamic driving force for chloride formation starting from the oxide catalyst and the vapor pressure of the formed chloride are two obvious descriptors. In this Review, we will use these descriptors to judge the catalyst's stability in the Deacon process (Section 3). We conclude this Review in Section 4 with a summary and a proposal of a potential Deacon catalyst that is motivated by the introduced volcano behavior in Sections 2 and 3: namely, La_2O_3.

2. CASE STUDY: HCl OXIDATION OVER RuO_2(110)-BASED MODEL CATALYSTS

The best-understood system for the Deacon process is the HCl oxidation over RuO_2(110)-based catalyst.[16,21−25] Upon exposure to HCl molecules at temperatures above 500 K, the stoichiometric RuO_2(110) surface transforms into a chlorinated surface where part of the bridging O atoms are replaced by chlorine.[15−18] The surface reaction of HCl oxidation therefore takes place over the surface chlorinated RuO_2(110). We will show that the overall reaction mechanism is governed by a delicate interplay of surface kinetics and thermodynamics, that is, the adsorption energies of reactants and reaction intermediates.

Mechanistic studies of the HCl oxidation over chlorinated RuO_2(110) were performed using DFT calculations[21,22] and HRCLS experiments;[22] similar DFT calculations were carried out for the HCl oxidation over stoichiometric RuO_2(110).[23] The Langmuir type kinetics of the HCl oxidation reaction over chlorinated RuO_2(110) is shown to be governed by the adsorption energies of the reaction intermediates (water, 120 kJ/mol; on-top Cl, 228 kJ/mol against Cl_2) (cf. Figure 1). The reaction mechanism of the HCl oxidation over chlorinated RuO_2(110) is summarized in Figure 1, and the energy diagram along the reaction coordinate is depicted in Figure 2.

All given energies in Figures 1 and 2 were determined by DFT calculations.[26] Dissociative adsorption of O_2 readily forms atomic O in an atop position of the 1f-cus Ru sites (O_{ot}). Actually, oxygen adsorbs first molecularly on the surface (by 40−120 kJ/mol), from where the dissociation is then activated by about 25 kJ/mol.[28] HCl molecules adsorb dissociatively with Cl sitting on-top of a 1f-cus Ru site, and the H atom is transferred to on-top O (or bridging O), forming a hydroxyl group: This adsorption process occurs without any noticeable activation barrier and is exothermic by 125 kJ/mol for the case of on-top O.[26] The next HCl molecule can form a second Cl_{ot} species and water; this process is exothermic by 178 kJ/mol (cf. Figure 2).

Adsorption of both oxygen and HCl require undercoordinated Ru atoms and are therefore competitive. The final production of surface water (H_2O_{ot}) can also occur via a H transfer between neighboring $O_{ot}H$ groups,[29] a process that is kinetically activated by 29 kJ/mol. Water desorption is endothermic by 120 kJ/mol (which equals the adsorption energy, since no further activation barrier has been found for water adsorption). This means that water desorption is activated by 120 kJ/mol.

The remaining Cl_{ot} species on the surface have to diffuse along the 1f-cus Ru rows to meet a second Cl_{ot} with which to recombine. This diffusion process is activated by 35 kJ/mol and

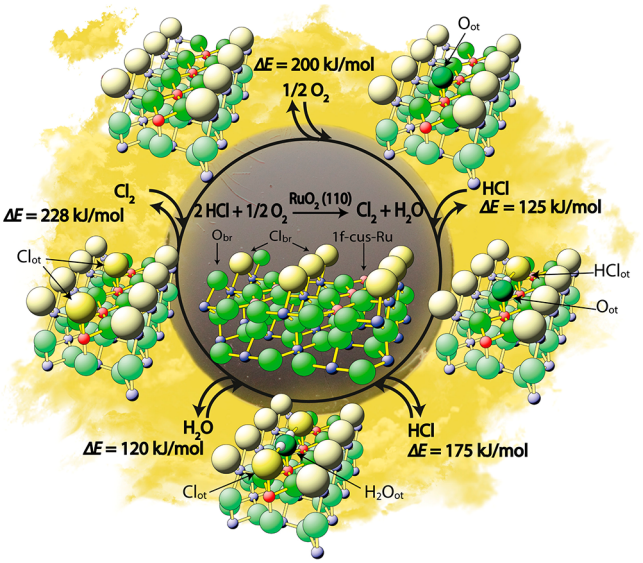

Figure 1. Catalytic cycle of the HCl oxidation over chlorinated RuO_2(110). In the schematic representation of RuO_2(110), the green balls are the oxygen atoms and the blue/red balls are Ru atoms in the bulk environment and (undercoordinated) at the surface, respectively. The chlorine atoms are represented by large yellow/green balls. In the HCl oxidation reaction (Deacon process) over RuO_2(110), both reactants O_2 and HCl adsorb dissociatively: O_2 and HCl cleavage proceeds in a homolytic and heterolytic way, respectively. Subsequently, surface oxygen is reduced to the byproduct water by H coming from dissociative HCl adsorption. Although the recombination of on-top Cl exhibits the highest activation barrier, 228 kJ/mol, the adsorption of oxygen is rate-determining for typical reaction conditions. In addition to surface reactions, the Deacon process is governed by the adsorption/desorption equilibria of Cl_2, O_2, H_2O, and HCl gases with the catalyst's surface; ΔE defines the adsorption energies. Copyright 2012, American Chemical Society.

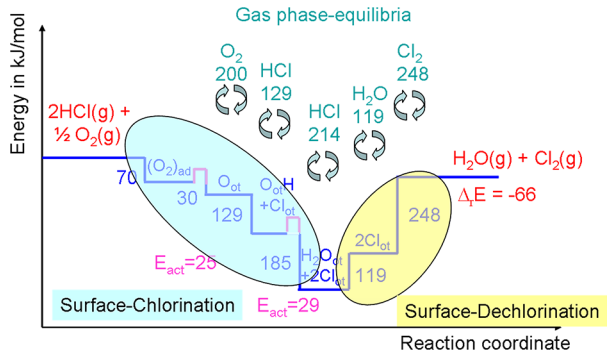

Figure 2. Energy diagram along the reaction coordinate for the HCl oxidation over chlorinated RuO_2(110), providing the adsorption energies in kJ/mol of the reaction intermediates (given in blue) and the activation energies (given in purple). Reaction energy: ΔE_r= −66 kJ/mol.[26] In addition, the equilibria between the gas phase and the surface are indicated, and the corresponding activation energies for desorption (green) are indicated in kJ/mol.

is therefore easily overcome at typical reaction temperatures of 500−600 K; however, we have to bear in mind that the interaction among direct neighboring Cl_{ot} is repulsive by about 20 kJ/mol, so Cl_{ot} recombination needs high surface Cl_{ot} coverage.[30]

The recombination of two on-top Cl to form the desired product Cl_2 constitutes the elementary reaction step with the

dx.doi.org/10.1021/cs300735e | ACS Catal. 2013, 3, 1034−1046

highest activation barrier of 228 kJ/mol.[22,26] This activation energy is given by the dissociative adsorption energy of Cl_2 (reverse reaction); dissociative adsorption of Cl_2 is not facing any kinetic barrier. This value for the activation barrier for chlorine desorption is higher than that reported by Lopez et al. for stoichiometric $RuO_2(110)$[23] (150 kJ/mol) but is in almost quantitative agreement with that of Studt et al.[21] (220 kJ/mol) for the chlorinated $RuO_2(110)$ surface. The DFT-calculated reaction energy ΔE_r of −66 kJ/mol at T = 0 K agrees reasonably well with the experimental value of −59 kJ/mol at T = 298 K.

For the case that most of the bridging O atoms are replaced by chlorine, the adsorption of HCl is tightly coupled to the surface concentration of on-top O, since HCl adsorbs molecularly too weakly (30−50 kJ/mol) and heterolytic splitting of HCl requires the presence of undercoordinated O atoms on the surface to accept the H-atoms from HCl splitting.

The energy profile along the reaction coordinate as shown in Figure 2 describes only one part of the reaction mechanism. In addition to these surface processes, the various gases—Cl_2, O_2, H_2O, and HCl—are in adsorption/desorption equilibrium with the catalyst's surface.[3,24] These equilibria result partly in reaction inhibitions. Water, for instance, can adsorb and desorb, thereby blocking active 1f-cus Ru sites, but it also leads to enhanced desorption of adsorbed Cl in the from of HCl by H-transfer from the adsorbed water molecule toward on-top Cl. If the partial pressure of Cl_2 is increased, the reaction rate also decreases. The reason for this product poisoning is related to blocking of the 1f-cus Ru sites by dissociative adsorption process of Cl_2, thus inhibiting dissociative oxygen adsorption. If most of the bridging O atoms are replaced by chlorine, then heterolytic dissociation of HCl is coupled to the oxygen adsorption, which in turn renders oxygen adsorption even more important for the reaction mechanism, underlining oxygen adsorption as the rate-determining step.

Only recently,[16] the first values for turnover frequencies have been reported for the HCl oxidation reaction over chlorinated $RuO_2(110)$ model catalysts. Reactivity experiments in a batch reactor indicate 0.6 Cl_2 molecules are produced per second and active site at 650 K (i.e., the turnover frequency TOF is 0.6 1/s), when starting with a reaction mixture of $P(HCl)$ = 2 mbar and $P(O_2)$ = 0.5 mbar. Microkinetic modeling was able to produce even a quantitative agreement with the experimental observed TOF = 0.6 1/s for the $RuO_2(110)$ surface.[24] In this microkinetic modeling,[24] which was based on ab initio calculated activation barriers but also on a mean field approach,[31,32] the surface was shown to be covered mostly by on-top Cl. This leads to a situation in which oxygen adsorption becomes rate-determining on $RuO_2(110)$, albeit the association of on-top Cl has the highest activation energy.

However, because of dimensional confinement on the $RuO_2(110)$ surface, a mean field approximation for microkinetic modeling is not justified.[31] For instance, on the stoichiometric $RuO_2(110)$ surface, trapped oxygen can be prepared by coadsorption of HCl and O_2. The term trapped oxygen describes oxygen atoms that are hindered to recombine to molecular oxygen by an inactive spectator/separator species, in this case, Cl_{ot} atoms. This steric hindrance of oxygen desorption may have profound implication on the reaction kinetics, allowing for configurational control in catalysis.[33] The trapped oxygen cannot be simulated by microkinetic modeling using mean field approach, but rather, it requires the application of kinetic Monte Carlo simulations.[31]

In conclusion, a full kinetic study of the HCl oxidation reaction over a catalyst surface such as $RuO_2(110)$ is a long-term task requiring kinetic Monte Carlo simulations because of 1-dimensional confinement, thus being not suitable for catalyst screening. However, from this case study, one can conclude that the energy landscape of the HCl oxidation is determined mainly by adsorption energies rather than by true kinetic barriers. This means activation energies in the catalyzed HCl oxidation reaction enter via an endothermic reaction step, such as the desorption of water, oxygen, and chlorine, whose reversed reactions—namely adsorption—are not kinetically hindered.

3. SEARCHING FOR INDICATORS/DESCRIPTORS TO ASSESS THE ACTIVITY OF DEACON CATALYSTS

3.1. BEP Relation. The Bronsted−Evans−Polanyi (BEP) relation[34,35] is an empirical rule that correlates the activation energy, E_{act}, and the involved reaction energy $\Delta_r H$ of an elementary reaction in a linear way $E_{act} = E^o_{act} + \gamma\Delta_r H$ (cf. Figure 3); E^o_{act} is the intrinsic activation barrier, and γ is the

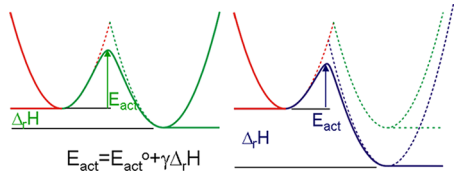

Figure 3. Schematic presentation of the BEP relation illustrating how activation energies, E_{act}, and reaction enthalpy (energies) $+\Delta_r H$ of elementary reactions are correlated.

reaction or transfer coefficient. The BEP relation thus allows for rationalizing observed variations in the catalytic activity of a specific reaction among various catalysts, and it allows us to estimate activation barriers. For instance, in the energy potential diagrams of an exothermic reaction in Figure 3, the activation energy for the elementary reaction A + B → C is lower the more negative the reaction energy is. For an endothermic reaction, the activation energy is often equal to or governed by the reaction energy of this process, assuming that the reverse reaction is not or only slightly activated. This kind of elementary reaction is frequently observed with the associative desorption of A_2 molecules, such as O_2 of Cl_2. Throughout the manuscript, we will not differentiate between energy and enthalpy (the differences are insignificant in the present discussion).

Over the past decade, the empirical BEP relation has been established quantitatively from DFT calculations for a variety of different reactions, starting with the pioneering work of Neurock[36] and others,[37−39] including N_2 activation,[40] CO oxidation over metal surfaces,[41] or BEP relations for transition metal oxides.[42]

3.2. Thermodynamic Approach. The first approach for assessing the activity of potential Deacon catalysts was pursued by Allen and co-workers in the mid 1960s.[20,43] The starting point was the original Deacon process over CuO, assuming that this reaction can be decomposed into two separate steps in which the catalyst undergoes a solid state redox cycle (cf. Figure 4). First, HCl reduces CuO to $CuCl_2$, during which water is formed as a couple-product. This chlorination process is exothermic. In the second step, $CuCl_2$ is reoxidized by molecular oxygen to recover CuO, thereby releasing the desired

dx.doi.org/10.1021/cs300735e | ACS Catal. 2013, 3, 1034−1046

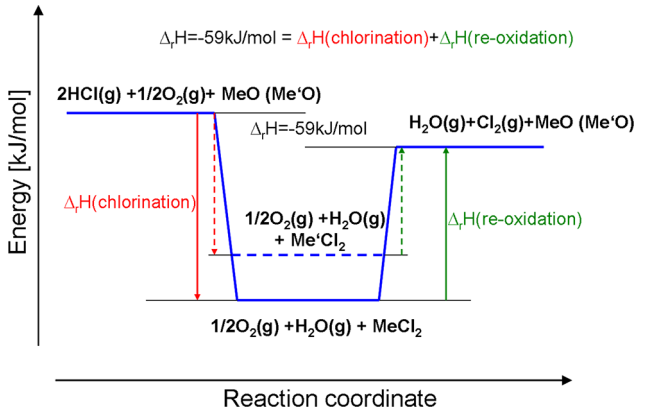

Figure 4. Decomposition of the catalyzed HCl oxidation reaction over CuO (original Deacon process) in a chlorination and a reoxidation step. Varying the catalyst material from Me to Me′ (broken lines) will lead to different reaction enthalpies or energies.

Cl_2 and closing the catalytic cycle. This reoxidation process can be considered an oxygen-driven dechlorination step. According to Hess' law, the reaction enthalpy is given by $\Delta_r H = -59$ kJ/mol = $\Delta_r H$ (chlorination) + $\Delta_r H$(reoxidation); in general, the chlorination step is exothermic and the reoxidation step is endothermic. Therefore, a strongly exothermic chlorination step leads inevitably to a prohibitively demanding (endothermic) reoxidation step, thus excluding such a material as a potential Deacon catalyst. This relation is illustrated in Figure 4. The reoxidation energy serves as the descriptor among various Deacon catalysts. For high reaction temperatures, when the reaction is close to equilibrium, the reaction energy for reoxidation (endothermic) is directly related to the activation energy (BEP relation), assuming that the reverse reaction for dissociative O_2 adsorption is not kinetically activated.

The scheme of decoupled reactions in the original Deacon process based on $CuO/CuCl_2$ has been materialized by the development of dual fluidized bed reactor systems for the efficient conversion of HCl to chlorine in which the chlorination and reoxidation process was performed in two separated reaction chambers, each with optimized temperature profiles and reaction conditions.[44,45]

On the basis of these early studies of Allen,[20] Hicham and Benson[19] investigated the thermodynamics of the Deacon process over several transition metal oxides as well as MgO and Al_2O_3; we have to note that RuO_2 was not considered in this report. The interrelation of chlorination and dechlorination of the catalyst was utilized to assess the activity of possible catalyst materials for the Deacon process.[19,20] From their study, Hisham and Benson[19] concluded that CuO is the only metal oxide that could undergo a complete catalytic cycle at temperatures below 700 K. Already in their original paper,[19] the authors pointed out that although a thermodynamic approach is useful, it can only provide constraints on possible catalytic reactions. In practice, kinetic parameters and physical properties may dominate.

Knowing this, the next obvious question is whether we could have predicted the RuO_2-based catalyst of Sumitomo Chemical on the basis of the available literature before the year 2000? The answer is yes (in principle), not on the basis of a rational design/concept in the form of a descriptor, but rather, by a direct comparison with the electrochemical oxidation of aqueous HCl.[46] Also for this reaction, RuO_2 supported on rutile TiO_2 has shown to be the most active and stable electrocatalyst in the early 1960s.[47]

We have to emphasize that for a heterogeneously catalyzed reaction mostly not the thermodynamics of bulk phases are of importance, but rather, the thermodynamics at the surface, that is, how strongly the reaction intermediates are bound to the catalyst surface. However, in many cases, the adsorption energy of intermediates correlates linearly with the corresponding bulk values of the reaction energies. Since over the past 4 years, several theoretical studies have been conducted on the Deacon process at various catalyst surfaces, including $RuO_2(110)$,[16,21−24] $TiO_2(110)$,[21,26] $RuO_2(110)-TiO_2(110)$,[26] $RuO_2(110)-SnO_2(110)$,[24] $CeO_2(111)$,[48] and CuCl,[49] we can try to adopt the thermodynamic approach of Allen and Benson to ab initio-derived binding energies of the reaction intermediates as summarized in Figure 5 and Table 1.

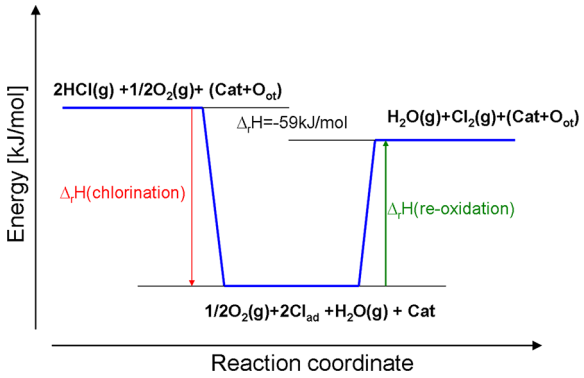

Figure 5. Simplified energy profile of the Deacon process over metal oxide catalysts considering only the involved thermodynamics of chlorination and reoxidation of the catalyst surface. Cat + O_{ot} is the catalyst with one on-top O atom sitting on the surface and Cat is the catalyst without this O_{ot} species.

Table 1. The Deacon Process Is Split into Two Separate Steps in Which the Catalyst Surface Undergoes a Redox Cycle: Chlorination and Re-Oxidation Step[a]

catalyst	$-\Delta_r H$ (chlorination), kJ/mol	$\Delta_r H$ (reoxidation), kJ/mol	ref
O_{ot} + c-RuO_2 (110)	194	128	22, 26
O_{ot} + RuO_2 (110)	200	95	23, 24
O_{ot} + RuO_2 (110)	160	90	21
O_{ot} + 1 ML RuO_2(110) on TiO_2(110)	195	130	26
O_{ot} + 1 ML RuO_2(110) on SnO_2(110)	180	130	24
O_{ot} + TiO_2 (110)	162	99	21, 26
$CuCl_2$	186	152	49
Cl_{ad} + H_{ad}/CeO_2(111)	90	30	48

[a]Corresponding reaction enthalpies of the chlorination and reoxidation step are given in kJ/mol. c-RuO_2(110): chlorinated RuO_2(110) surface where the bridging O atoms are replaced by chlorine.

The catalysts are not the bulk metal oxides, but rather, metal oxide surfaces that are covered partly by atomic oxygen (Cat + O_{ot}) (cf. Figure 6b) or, as in the case of $CeO_2(111)$, which consists of $CeO_2(111)$, with one of the surface oxygen atoms replaced by chlorine and other surface oxygen atoms transformed to hydroxyl groups.[48]

From Table 1, we could infer that $CeO_2(111)$ is the most efficient catalyst, since the reoxidation step is the least

dx.doi.org/10.1021/cs300735e | ACS Catal. 2013, 3, 1034−1046

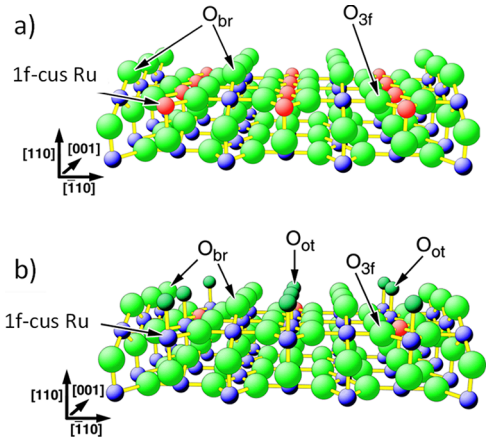

Figure 6. Ball and stick model of the stoichiometric $RuO_2(110)$ surface (a) and the oxygen exposed $RuO_2(110)$ surface (b), where most of the undercoordinated 1f-cus Ru sites are occupied by on-top O (O_{ot}); this latter surface corresponds to Cat + O_{ot} in Figure 3. The big green balls are the oxygen atoms, the small blue and red balls are the Ru atoms. At the stoichiometric $RuO_2(110)$ surface, there are two types of undercoordinated atoms: the bridging O atoms (O_{br}) and the 1f-cus Ru site. 1f-cus stands for one-fold coordinatively unsaturated site.

endothermic one among the considered catalysts, and all others are similarly active. None of these implications is correct when compared with experimental studies. The most efficient catalyst is O_{ot}–$RuO_2(110)$. $TiO_2(110)$ is not active at all, since oxygen dissociation is endothermic by 219 kJ/mol.[21,26] And $CeO_2(111)$ is much less active than RuO_2, since adsorbed chlorine has to be activated for Cl_2 liberation from the surface, which is endothermic by 200 kJ/mol.[48] However, $CuCl_2$ reveals a higher activation energy for chlorine release than RuO_2, as is also experimentally observed.

A more elaborate energy diagram is presented in Figure 7. In particular, the reoxidation process is split into an oxidation step

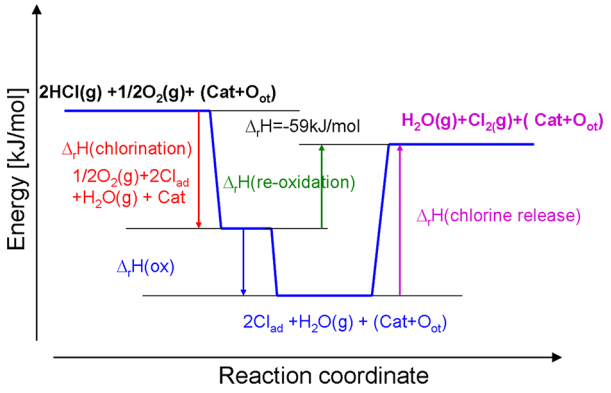

Figure 7. Simplified energy profile of the Deacon process over metal oxide catalysts considering only the involved thermodynamics of chlorination, oxidation (ox) of the catalyst, and the chlorine release from the surface. "Cat" stands for the catalyst.

(oxygen adsorption) and the liberation of chlorine from the surface (chlorine release). Theoretical studies[21] suggest that the oxidation step, in particular the dissociation energy of O_2, is a promising descriptor for ranking the activity of potential Deacon catalysts (cf. Sections 3.4 and 3.5).

At high reaction temperature, the apparent activation energy is given by Δ_rH(reoxidation), whereas at moderate temperature, the activation energy is given by the Δ_rH(chlorine release). Again, notice that the reaction energy for chlorine release is mostly endothermic so that the activation energy for chlorine release is given by the reaction energy (assuming that the reverse, i.e., dissociative Cl_2 adsorption, reaction is not kinetically hindered).

From Figure 7 and Table 2, the actual activity of the considered catalysts can be mostly properly estimated. For the

Table 2. The Deacon Process Is Split into Three Separate Surface Reaction Steps: Chlorination, Oxidation and Chlorine Release[a]

catalyst	$-\Delta_rH$(chlor), kJ/mol	$-\Delta_rH$(ox), kJ/mol	ΔH(Cl_2 release)	ref
O_{ot} + c-RuO_2 (110)	194	100	228	22, 26
O_{ot} + RuO_2 (110)	200	60	155	23, 24
O_{ot} + RuO_2 (110)	160	30	120	21
O_{ot} + 1 ML RuO_2(110) on TiO_2(110)	195	118	248	26
O_{ot} + 1 ML RuO_2(110) on SnO_2(110)	180	100	180	24
O_{ot} + TiO_2 (110)	162	−219!!	−120	21, 26
$CuCl_2$	186	−88!!	64	49
Cl_{ad} + H_{ad}/CeO_2(111)	90	125	150	48

[a]Corresponding reaction enthalpies are given in kJ/mol. c-RuO_2(110): chlorinated RuO_2(110) surface where the bridging O atoms are replaced by chlorine.

$CuO/CuCl_2$ catalyst, the oxidation step is inhibiting the HCl oxidation reaction. Dissociative adsorption of oxygen is activated by 88 kJ/mol. From a thermodynamic point of view, $CeO_2(111)$ would still be quite an active catalyst, since Cl_2 release is endothermic by only 150 kJ/mol and therefore similar to those values of RuO_2-based catalysts.[2] This contradiction with experimental observation is not surprising because the reaction mechanism is also considered to be profoundly different.[48] From Table 2, it is also evident that DFT calculations of the same reaction (e.g., Deacon over $RuO_2(110)$) can largely vary, rendering ab initio calculations less conclusive than frequently expected. This aspect is discussed by authors developing DFT methods.[50]

Altogether, simple thermodynamics is able to largely capture the trend of activity variations among various Deacon catalysts, but this section also shows that this approach may lead to erroneous conclusions about the expected activity, as seen, for instance, with CeO_2.

3.3. Oxygen Activation: $^{16}O_2/^{18}O_2$ Exchange Reaction.

Oxidation catalysts for the Deacon process must fulfill two important functions: the activation of HCl and the activation of molecular oxygen. In general, the latter step is the bottleneck and can be probed and estimated from $^{16}O_2/^{18}O_2$ exchange reaction experiments.[51,52] Therefore, an alternative indicator or descriptor for the catalytic activity of an oxide catalyst in the Deacon process could be the relative ranking for the exchange of $^{16}O_2/^{18}O_2$ with the oxide surface normalized, for instance, to 500 °C.[52]

From Figure 8, one can imply that IrO_2, CuO, and RuO_2 would actually be the most active Deacon catalysts and Nb_2O_5 would be the least active catalyst among the various oxide catalysts. Both conclusions are roughly reconciled with published activity data for the Deacon process;[16,21−24,27,53]

dx.doi.org/10.1021/cs300735e | ACS Catal. 2013, 3, 1034−1046

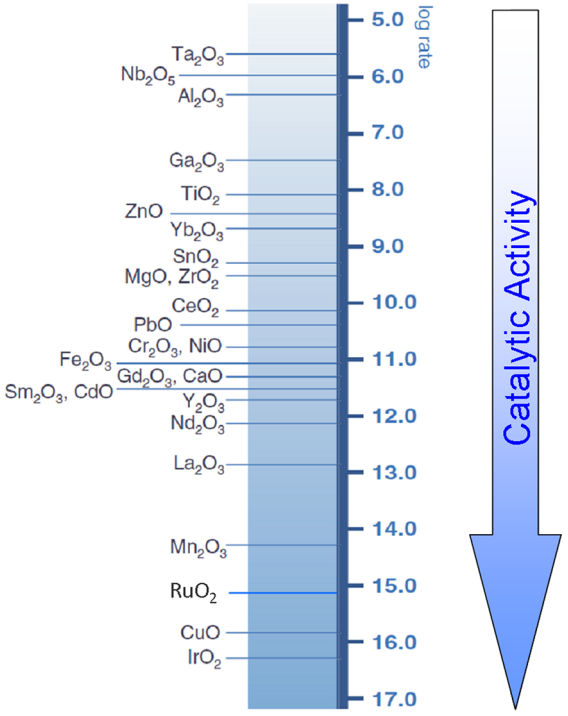

Figure 8. Relative ranking order for the exchange of $^{16}O_2/^{18}O_2$ with oxide surfaces normalized at 500 °C.[52] MoO_3 is not included because $^{16}O_2/^{18}O_2$ exchange is very rapid, occurring by a different mechanism. Reproduced with permission from reference 52. Copyright 2003, Springer.

however, among the three catalysts—CuO, RuO_2, and IrO_2—RuO_2 has shown to be outperforming,[1,2] which is not directly retrieved by the $^{16}O_2/^{18}O_2$ exchange propensity in Figure 8. Cr_2O_3 is also an efficient (but not very stable) catalyst for the Deacon process,[11,54] although the $^{16}O_2/^{18}O_2$ exchange rate is only in the medium range. According to Figure 8, other potential candidates for Deacon catalysts are La_2O_3 and Mn_2O_3. As mentioned before, in addition to activity, stability is a major issue for the Deacon process. One could expect that the stability of the oxidation catalyst might be inversely related to the $^{16}O_2/^{18}O_2$ exchange rate. The more easily the exchange of oxygen occurs in the catalyst, the easier the in-depth chlorination of the catalyst might be possible. Summarizing, we may conclude that the $^{16}O_2/^{18}O_2$ exchange rate is helpful but not conclusive in identifying potential catalysts for the Deacon process.

3.4. Thermodynamics: Transformation from Lower to Higher Oxides. The catalytic activity is to a large extent determined by the binding strength of the reaction intermediates to the catalyst's surface (Sabatier principle). Because the binding energies of reaction intermediates are difficult to measure, other descriptors have been searched for. One example is the use of the standard enthalpy of lower to higher oxide transformation ($MO_x \rightarrow MO_{x+1}$).[51,55−57]

Trasatti suggested, for instance, in the discussion of the electrocatalytic oxygen evolution reaction (OER) that the O-metal bonding is a decisive parameter to judge whether an electrode material is a good catalyst for OER. Among the various oxides, Trasatti[58,59] found a kind of volcano curve for the electrocatalytic activity for the OER as a function of the standard enthalpy of lower-to-higher oxide transformation (cf. Figure 9).

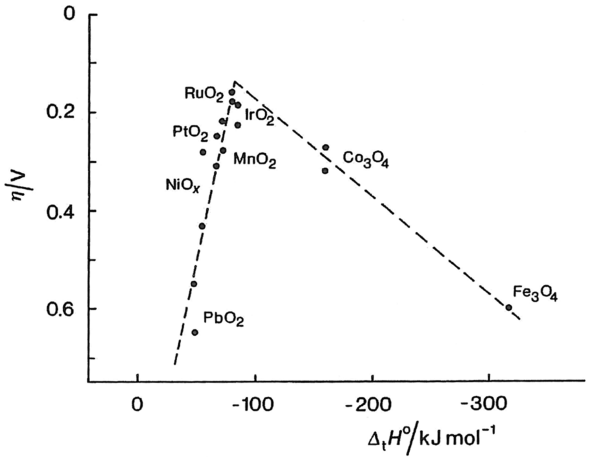

Figure 9. Activity (expressed as overpotential η at 0.1 mA/cm^2) for O_2 evolution (OER) on various electrodes as a function of standard enthalpy $\Delta_f H°$ of lower-to-higher oxide transformation.[57,58] Reproduced with permission from reference 57. Copyright 1984, Elsevier.

RuO_2 lies close to the apex of this volcano curve, thus being the most active OER catalyst. This volcano behavior can be rationalized in the following way: On the left-hand side of the volcano curve, the O−metal bond is too weak, and accordingly, reaction intermediates absorb too weakly to allow for efficient OER (BEP relation: dissociation of water becomes rate-limiting). On the right-hand side of the volcano curve, the O−metal bond is too strong, and therefore, the reaction intermediates adsorb too strongly (BEP relation: activation energy increases) to allow for efficient OER. Removal of the oxygenated species becomes rate-limiting for OER. Right at the center of the volcano plot, where the O−metal bond is neither too strong nor too weak (Sabatier principle), the optimum O−metal bond strength is realized by RuO_2. In general, it has been observed that materials that are active for OER are also active in the chlorine evolution reaction (CER).[58]

In a screening experiment for Deacon catalysts,[60] it was shown that the catalytic activity of electrode materials suitable for CER are equally good for catalysts for the Deacon process. Therefore, a similar volcano plot as shown in Figure 9 is expected for the Deacon process and has, indeed, already been observed in theoretical calculations, at least for rutile-type oxides.[21,25,61,62]

3.5. Theory: Volcano Behavior with O_2 Dissociation Energy Being the Descriptor. Studt et al.[21] combined BEP relations[36−39] and scaling relations[63,64] with microkinetic modeling of the HCl oxidation reaction for various transition metal oxides to derive volcano curves for the activity over various transition metal oxide catalysts with rutile structure. The fact that molecules with strong or moderate intramolecular bonds dissociate without any substantial barriers on rutiles makes these oxides promising catalysts for the activation of diatomic molecules.

The theoretical study by Studt et al.[21] clearly indicates that the dissociation energy of O_2 given by the reaction energy of $O_2(g) \rightarrow 2O_{ot}$ (cf. Figure 6) is linearly correlated with the adsorption energy of other reaction intermediates on the surface, such as on-top Cl, water, and OH (scaling relations), and these adsorption energies are linearly related to reaction barriers (BEP relation). Therefore, the activity can be plotted as a function of only a single parameter—namely, the dissociation energy of O_2) $\Delta E_{diss}(O_2)$—resulting in a volcano-shaped

dx.doi.org/10.1021/cs300735e | ACS Catal. 2013, 3, 1034−1046

relationship between catalytic activity and the calculated oxygen adsorption energy (cf. Figure 10). The studies of Studt et al.[21] disclosed impressively that the activity of $RuO_2(110)$ is already very close to the optimum value (cf. Figure 10).

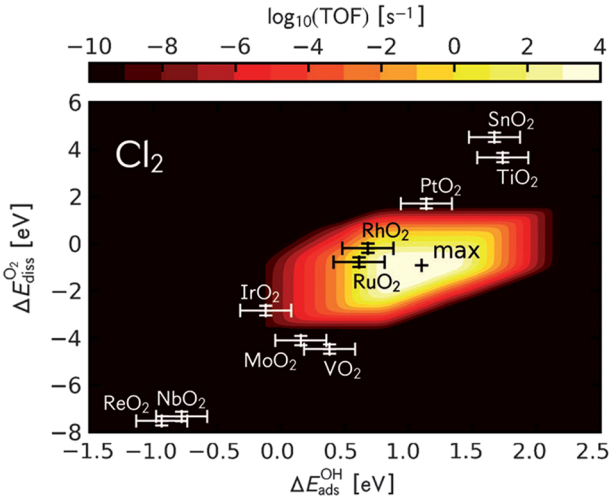

Figure 10. Volcano plots with TOFs (turnover frequency) plotted as a function of $\Delta E_{diss}(O_2)$ and the adsorption energy of OH ($\Delta E_{ads}(OH)$) for HCl, oxidation. Clearly, the activity is uniquely determined by $\Delta E_{diss}(O_2)$. Reaction conditions: T = 573 K, $p(O_2)$ = 0.6 bar, p(HCl) = 0.3 bar, $p(H_2O)$ = 0.05 bar, and $p(Cl_2)$ = 0.05 bar.[25] Reproduced with permission from reference 25. Copyright 2012, John Wiley and Sons.

The volcano curve in Figure 10 can be rationalized in the following way. If the O_2 dissociation energy is highly exothermic, then chlorine adsorbs strongly on the surface so that the liberation of Cl_2 restricts the activity, such as observed with $IrO_2(110)$. However, for surfaces that bind oxygen too weakly, dissociative oxygen adsorption becomes rate-limiting, as encountered, for instance, with $TiO_2(110)$.[21] Right between these antipodes, where the metal−oxygen binding energy is moderate (Sabatier principle), the activity is also the highest.

We have to recall that for many oxide surfaces, defect sites represent the active centers for oxidation reactions. In the case of $RuO_2(110)$[65] or $IrO_2(110)$,[21,66] the perfect surface is already active in the Deacon process, but the perfect $TiO_2(110)$ is not active at all because the activation of oxygen is prohibitively energy demanding. However, if bridging oxygen vacancies are present at the $TiO_2(110)$ surface, the oxygen activation is facilitated.[67] Unfortunately, the important role of defects has not been considered in the work of Studt et al.[21,25]

3.6. Experiment: Volcano Behavior with O_2 Dissociation Energy Taken As the Descriptor. Encouraged by the work of Studt et al,[21,25] we construct in this section a volcano plot for experimentally determined activity data as a function of the theoretically derived dissociation energy serving as the descriptor. At least for transitions metal oxides with rutile structure, this choice of descriptor is justified. However, for other oxides, the dissociation energy of O_2 is reasonable, as well, as long as the Cl−metal bond is correlated with the O−metal bond and the chlorine release is the elementary reaction step with the highest activation barrier. We do not intend to corroborate the chosen descriptor for other oxide catalysts, but rather, we assess the chosen descriptor just by the fact that experimental activity data will form a volcano curve and that the derived volcano curve is able to predict/suggest the activity of catalysts when the dissociation energy of O_2 is known.

To enlarge the database for the chosen descriptors, we go back to the work of Man et al..[68] In this study, the universality of the oxygen evolution reaction among various oxide surfaces was discussed. One can easily show for the rutile transition metal oxides that between the adsorption energies of atomic O in the work of Man et al. (supplement of ref 68) and the dissociation energy of O_2 of Studt et al., there exists a linear relationship.[69] This linear relation can then be utilized to convert the adsorption energies of Man et al. for other metal oxides in terms of O_2 dissociation energies, $\Delta E_{diss}(O_2)$, in Table 3. In addition, other dissociation energies of O_2 on oxide surfaces found in the literature are compiled in Table 3.

For a correlation of the activity data with the dissociation energy of oxygen $\Delta E_{Diss}(O_2)$, the available activity data of catalysts that consist of a powder of a single component were analyzed. In ref 70, a series of powder catalysts was investigated under comparable conditions. Because of the strong product inhibition, only data collected at ambient pressure and low conversion were considered. The activity is expressed as space−time−yield (STY) in g_{Cl_2}/g_{cat}·h and refers to the mass of catalyst. The ranking in the activities is $RuO_2 \gg Cr_2O_3 > CeO_2 > CuO > MnO_2$, although RuO_2 was tested at 573 K and the others were tested at 723 K. These activities were converted to a temperature of 673 K applying the apparent activation energies of the individual catalysts. To exclude the influence of different particle sizes, the STY data were further converted to surface-related rates in mol$(Cl_2)/m^2$·s by a division by the given BET surfaces measured after testing the catalyst. Further data were included from a screening experiment with alumina-supported nanoparticles of about 10 nm diameter of different metal oxides.[60] Under the same test conditions as described in ref 70 and a temperature of 673 K, the experiment showed the same ranking for RuO_2, CeO_2, and CuO as was found for the powder catalyst. The activities for NiO and Co_2O_3 were included according to their ratio to the activity to RuO_2. With the same procedure, the surface-related activity of V_2O_5 was obtained from data described in ref 82.

For the O_2 dissociation energies in Figure 11, we used mostly those values determined in Norskov's group.[21,25,68] This choice bears the advantage that the relative energies among the various catalyst systems are properly taken into account. The absolute values of the dissociation energies of O_2 may differ significantly among different DFT studies, as revealed for the case of $RuO_2(110)$.

Figure 11 illustrates impressively how much more active RuO_2 is in comparison with other potential Deacon catalysts, such as CuO or Cr_2O_3. However, if one considers that the activity of CuO and Cr_2O_3 can compete with that of RuO_2, from an economic point of view (considering the price of the catalyst material), then NiO and Co_3O_4 are promising potential Deacon catalysts, as well, which should be studied in more detail in the future.

4. SEARCHING FOR INDICATORS/DESCRIPTOR FOR ASSESSING THE STABILITY OF DEACON CATALYSTS

One of the major problems with Deacon catalysts is the lack of stability of the catalysts under the harsh conditions of the HCl oxidation reaction. There are various kinds of instabilities observed with Deacon-type catalysts, including sintering of the

dx.doi.org/10.1021/cs300735e | ACS Catal. 2013, 3, 1034−1046

Table 3. Reactivity Data (experimental and theoretical) for the HCl Oxidation Reaction Given in STY (space time yield) and ($\Delta E_{diss}(O_2)$) Values That Can Be Used As the Descriptor in the Experimental Volcano Plot Depicted in Figure 11[a]

system	reactivity STY of Cl_2 (g Cl_2 h^{-1} g_{cat}^{-1})	remarks	ref
CeO_2	0.77	flow reactor; 1 bar, 723 K	48, 70
		BET: 106 → 26 m^2/g	
		E_{app} = 90 kJ/mol	48
CeO_2(111) with O vac.		$\Delta E_{diss}(O_2)$ = −230 kJ/mol (theory)	
Co_3O_4(100)		$\Delta E_{diss}(O_2)$ = 60 kJ/mol	71, 72
Co_3O_4		$\Delta E_{diss}(O_2)$ = +30 kJ/mol	68
Cr_2O_3	1.15	flow reactor; 1 bar, 723 K	70
		BET: 10 m^2/g	
		E_{app} = 96 kJ/mol	
CrO_2(110)		$\Delta E_{diss}(O_2)$ = −200 kJ/mol (theory)	68
CuO	0.15	flow reactor; 1 bar, 723 K	70
$CuCl_2$	0.40	BET: 2 m^2/g	70
		light-off T: 625 K	
Cu_2O(111)[b]		$\Delta E_{diss}(O_2)$ = −200 kJ/mol	73
CuCl(111)		$\Delta E_{diss}(O_2)$ = −120 kJ/mol	74
$CuAlO_2$ delafossite	conversion: 25%	fixed bed reactor: T = 653 K, 1 bar, 10 vol % HCl, 40 vol % O_2	75
		E_{app} = 100 kJ/mol	
		stable under reaction conditions, activity similar to CuO	
IrO_2(110)	negligible; 573 K, theory	$\Delta E_{diss}(O_2)$ = −250 kJ/mol	21
La_2O_3(001)		$\Delta E_{diss}(O_2)$ = +50 kJ/mol	76
MnO_2	0.03	flow reactor; 1 bar, 723 K	70
		BET: 1 m^2/g	
		also less active in OER than RuO_2, IrO_2	
MnO_2(110)		$\Delta E_{diss}(O_2)$ = +20 kJ/mol (theory)	68
NbO_2(110)	negligible; 573 K, theory	$\Delta E_{diss}(O_2)$ = −720 kJ/mol	21
NiO		$\Delta E_{diss}(O_2)$ = −60 kJ/mol	68
PtO_2(110)	negligible; 573 K, theory	$\Delta E_{diss}(O_2)$ = +180 kJ/mol	25
RhO_2 (110)		$\Delta E_{diss}(O_2)$ = 0 kJ/mol	68
RuO_2	5.09	flow reactor; 1 bar, 573 K	36
		BET: 10 m^2/g	
		E_{app} = 72 kJ/mol	
		light-off T (10%): 500 K	
RuO_2(110)		$\Delta E_{diss}(O_2)$ = −70 kJ/mol (theory)	25
RuO_2(110)		$\Delta E_{diss}(O_2)$ = −200 kJ/mol(theory)	77, 78
RuO_2/r-TiO_2	1.19	fixed bed reactor	79
RuO_2/a-TiO_2	0.83	BET: 140 m^2/g (r-TiO_2), 575 K	
		100 m^2/g (a-TiO2), 600 K	
1 ML RuO_2 on TiO_2(110)		$\Delta E_{diss}(O_2)$ = −236 kJ/mol	26
SnO_2(110)	negligible, expt.	$\Delta E_{diss}(O_2)$ = +450 kJ/mol	24, 68, 80
TiO_2(110)	negligible, expt.	$\Delta E_{diss}(O_2)$ = +380 kJ/mol	21, 81
V_2O_5	0.04	T = 558 K, 1 bar, 15% HCl, 85 vol % air	82, 83
	0.33	T = 643 K	
		E_{app} = 40 kJ/mol	
V_2O_5(001)		vanadyl: $\Delta E_{diss}(O_2)$ = −400 kJ/mol	84
		$\Delta E_{diss}(O_2)$ = −420 kJ/mol	
VO_2(110)	negligible, 573 K, theory		25, 68

[a] E_{app} stands for the experimentally derived apparent activation energy. BET corresponds to the active surface area given in m^2 per gram catalyst as determined by physisorption measurements. [b] Under typical reaction conditions, cuprous Cu_2O is the stable phase rather than CuO, exposing free cus-Cu sites for oxygen and HCl adsorption.[85,86]

particles, as observed with a loss of BET area (RuO_2-based catalyst;[53] CeO_2-based catalyst[48,81]) and loss of the active component by volatilization (CuO/$CuCl_2$ or Cr_2O_3[53]). In both cases, the underlying process requires a volatile metal species formed under the specific reaction conditions. Since the employed oxide catalysts are in most cases not volatile at the reaction temperature, another volatile species has to be formed during the reaction, most likely metal chlorides or oxychlorides.

To form volatile metal chlorides, two requirements have to be fulfilled: first, the bulk chlorination has to be thermodynamically feasible, and second, the partial pressure of the formed metal chlorides has to be high enough at reaction temperatures. Two thermodynamic characteristics directly reflect these properties: namely, the formation energy for the chloride in comparison with the formation energy of oxide formation (corresponding to the thermodynamic driving force for chloride formation starting from the oxide) and the melting

dx.doi.org/10.1021/cs300735e | ACS Catal. 2013, 3, 1034−1046

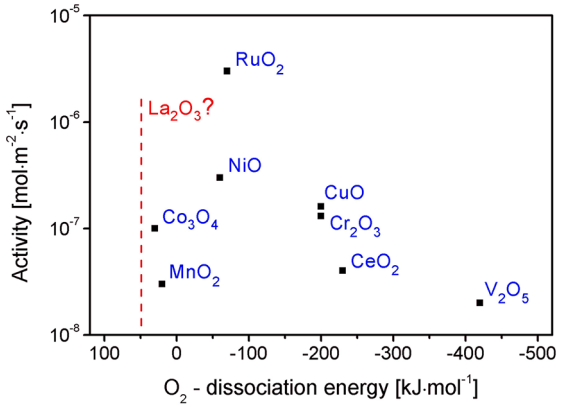

Figure 11. Experimental volcano curve. Activity tests in tubular reactor at 1 bar, HCl/O_2 >2 balanced to 1 bar with nitrogen; conversion <10%, T = 673 K. The activity is given in mol/(m^2·s). Experimental activity data taken from literature: RuO_2,[70] V_2O_5,[82] Cr_2O_3,[70] CeO_2,[48] CuO,[70] NiO,[60] MnO_2,[70] and Co_3O_4.[60] The descriptor is the O_2 dissociation energy as determined by DFT calculation and compiled in Table 3.[21,25,68]

and boiling points of the metal chlorides, respectively. Both quantities are compiled in Table 4. Of course, this is a crude approximation because, in general, not a pure metal chloride is formed under reaction conditions, but rather, an oxychloride whose thermodynamic data are largely unknown. Also included in Table 4 are the expected and the observed stability (where available form the open literature).

From Table 4, one can recognize that for most of the metal oxides, the stability under Deacon-reaction conditions is correctly described; that is, the expected thermodynamic stability based on the formation energies of oxides and chlorides as well as melting/boiling points of chlorides agrees reasonably well with the experimentally observed stability. There are, however, also two prominent exceptions, namely, Mo oxides and Cr oxide, for which the "expected" stability is difficult to access. Experimentally, MoO_3 is unstable and completely vaporizes at 250 °C.[19] From Table 4, Mo oxides are expected to be stable for T < 500 °C as long as no $MoCl_5$ is formed. If $MoCl_5$ is formed, then this chloride species is quite volatile, even at 200 °C. With Cr oxides, a similar problem is encountered. Starting from Cr oxides, the driving force for the formation of chlorides is high enough to proceed; however, only $CrCl_4$ is volatile at low temperatures, whereas the other Cr chlorides evaporate only above 700 °C.

In some cases, the formation of volatile metal chlorides is only moderately favored by their thermodynamic driving force. Here, the equilibrium between stable oxides and volatile chlorides may be controlled by the partial pressure of oxygen in the reaction mixture. With an excess of oxygen in the feed mixture, not only the conversion of HCl is increased in comparison to a stochiometric feed, but also the composition of the catalyst surface is shifted to the more stable oxide species. For catalysts with such a sensitive stability behavior, a depletion of oxygen in the catalyst bed has to be avoided. This may be achieved by an appropriate oxygen excess in the feed or by a dosing strategy for HCl, where this is introduced into the reactor only stepwise.

Altogether, the stability of potential Deacon catalysts can be surprisingly well predicted on the basis of the formation energies of oxides and chlorides as well as the melting/boiling points of the chlorides.

5. CONCLUDING REMARKS

Not only theoretically (cf. Figure 10) but also experimentally (cf. Figure 11), a volcano curve for the activity of oxide catalysts in the oxidation of HCl (Deacon process) can be designed when the O_2-dissociation energy on these oxide surfaces is chosen as the descriptor. Already the ranking of experimental activity data in the form of a volcano curve (cf. Figure 11) corroborates the O_2 dissociation energy to be a reasonable descriptor. For various oxidation reactions, RuO_2 is found to be at the apex of such volcano curves because its oxygen dissociation energy is already at the optimum. Therefore, a single metal oxide catalyst may not be improved according to the calculations performed in Norskov's group.[21,68]

However, bifunctional catalysts such as binary or ternary mixtures of oxides may improve their activity in the Deacon process when compared with single oxides. For example, in the NH_3 synthesis, it has been shown that a mixture of two elements, one from the left side of the volcano curve and the other from the right side, can further improve the catalytic performance.[91] A similar strategy may also be applied for the Deacon process. Looking at the experimental volcano plot in Figure 11, CuO is on the left side of the volcano, and Co_2O_3 or La_2O_3 (Table 3) is on the right side; therefore, a mixture of CuO + Co_3O_4 or a mixture of CuO + La_2O_3 may result in an improved Deacon catalyst.

Future research in the Deacon process should be devoted to the determination of activities of other oxide materials for which the calculated O_2 dissociation energies are known (cf. Table 3). Furthermore, we need additional ab initio calculations of O_2 dissociation energies for other oxide materials and also for oxides with defects. This will lead to an enlarged database for the volcano curve presented in Figure 11 so that stronger conclusions and design ideas can be derived, for example, for the selection of suitable dopant materials.

The stability of a Deacon catalyst can be assessed on the basis of thermodynamic data for the formation of the chlorides and the volatility of these chlorides under reaction conditions (characterized by the melting and boiling temperatures of the chloride). From this analysis (cf. Table 4), it is suggested that La_2O_3 is a stable catalyst that may also be active, as indicated by a substantial value for the oxygen exchange propensity (cf. Figure 8). In addition, an O_2 dissociation energy of +50 kJ/mol (cf. Table 3) is determined for La_2O_3, which is close to the optimum value realized by RuO_2 (cf. Figure 11). Preliminary activity experiments in our group support this suggestion. La_2O_3 is, indeed, a remarkably active Deacon catalyst. A commercially available La_2O_3 powder with a BET surface of 6 m^2/g was tested at 400 °C with 0.5 g of catalyst powder (200–300 μm), and 80 mL/min of a reactant mixture of $HCl/O_2/N_2$ = 1:1. A production rate of 1×10^{-8} mol Cl_2 m^{-2} s^{-1} was determined by titration of the Cl_2 gas captured from the reactor effluent gas in an absorption column. This value agrees nicely with a value that would be predicted from the oxygen dissociation energy on the basis of the vulcano plot in Figure 11. This finding lends further support to the chosen descriptor. Deposition of this material on the surface of an appropriate support material could greatly improve the performance of La_2O_3 as a Deacon catalyst, as is seen for RuO_2 if unsupported[70] and supported[24] RuO_2 catalysts are compared.

Finally, the stability of a Deacon catalyst depends critically on the process parameters, such as the reaction temperature and the reaction feed composition. The higher the required reaction

dx.doi.org/10.1021/cs300735e | ACS Catal. 2013, 3, 1034–1046

Table 4. List of Formation Energies of Oxides and Chlorides As Well As Melting/Boiling Points of Chlorides[a]

oxide formation energy, kJ/mol	metal chloride formation, kJ/mol	melting/boiling points (°C)	stability against formation of volatile chlorides: expected or experimentally (expt) observed stability
AgO, −62	AgCl, −127	455/1550	chloride formation, high; T > 450 °C; high vapor pressure expected to be low, T > 450 °C expt, −
CeO_2, −1090 boiling point 2400 °C	$CeCl_3$, −1060	848/1727	chloride formation, medium; T < 600 °C; very low vapor pressure expected, very high expt, very high; T < 600 °C[88,89]
CoO, −238	$CoCl_2$, −313	735/1049	chloride formation, medium to high; T > 700 °C; low vapor pressure (dep. on the water content)
Co_3O_4, −892	$CoCl_2 \cdot 1H_2O$	140/−	expected to be low; >200 °C
	$CoCl_2 \cdot 2H_2O$	100/−	expt, −
	$CoCl_2 \cdot 6H_2O$	86 (100)	
CrO_3, −590; CrO_2, −599 Cr_2O_3, −1140	$CrCl_4$ $CrCl_3$, −557 $CrCl_2$, −396	−28 (decomp)/− 1152/− 815/1122	chloride formation, medium/low vapor pressure expected to be high expt, low; T > 400 °C[11,48]
Cu_2O, −169 CuO, −157	CuCl, −137 $CuCl_2 \cdot 2H2O$, − $CuCl_2$, −220	430/1490 1083/2595 300 °C decomp./−	chloride formation, high; T > 400 °C; high vapor pressure expected, low; T > 400 °C expt, low; T > 400 °C[90]
FeO, −272 Fe_2O_3, −824 Fe_3O_4, −1118	$FeCl_3$, −400 $FeCl_2$, −342	304/319 subl. 120 °C 676/1012	chloride formation, high; T > 300 °C; high vapor pressure expected to be low for T > 120 °C expt, −
IrO_2, −274	$IrCl_3$, −245	763/−	chloride formation, medium; T < 600 °C; low vapor pressure expected to be high for T < 600 °C expt, −
La_2O_3, −1794	$LaCl_3$, −1072	860/1812	chloride formation, low; T < 800 °C; low vapor pressure expected to be high; T < 800 °C expt, −
MnO, −385 Mn_2O_3, −960 MnO_2, −529	$MnCl_4$, − $MnCl \cdot 4H_2O$ $MnCl_2$, −482	650/− 58/− −/−	chloride formation, medium; T < 600 °C; low vapor pressure expected to be high for T < 500 °C expt, less bulk chlorination than with CuO[70]
MoO_3, −746 MoO_2, −589	$MoCl_6$ $MoCl_5$, −528 $MoCl_4$, −481 $MoCl_3$, −387 $MoCl_2$, −282	795/1155 194/− 552/− −/− −/−	chloride formation, low; T < 500 °C; low vapor pressure expected, high for T < 500 °C expt, MoO_3; very low; T > 250 °C; completely evaporized[19]
Nb_2O_5, −190 NbO_2, −800 NbO, −406	$NbCl_5$, −796 $NbCl_4$, −695 $NbCl_3$, −586 Nb_3Cl_8, −538	205/248 800 (decomp)/275 °C (subl.) vapor pressure, 10^{-4} mbar −/− −/−	chloride formation, medium; T < 500 °C; low vapor pressure expected to be low; T > 200 °C expt, −
NiO, −240; Ni_2O_3, −490	$NiCl_2$, 305 $NiCl_2 \cdot 6H_2O$	1001/− 140/−	chloride formation low; Ni chloride only volatile below 200 °C if hydrated expected, ambiguous expt, Ni is very stable
RuO_2, −305	$RuCl_3$, −250	500/−	chloride formation, medium; T < 500 °C; low vapor pressure expected, high for T < 350 °C expt, high; T < 350 °C; low, T > 450 °C[81]
SnO_2, −578	$SnCl_2$, −325	245/620	chloride formation, low; T > 300 °C; high vapor pressure

dx.doi.org/10.1021/cs300735e | ACS Catal. 2013, 3, 1034−1046

Table 4. continued

oxide formation energy, kJ/mol	metal chloride formation, kJ/mol	melting/boiling points (°C)	stability against formation of volatile chlorides: expected or experimentally (expt) observed stability
	$SnCl{\cdot}2H_2O$		expected to be low, medium for T > 300 °C expt, low for T > 300 °C[24]
TiO_2, −945 Ti_2O_3, 1537 TiO, −517	$TiCl_4$, −750 $TiCl_2$, −477	−24/136 1035/1500	chloride formation, low; T > 700 °C; low vapor pressure expected to be high; T < 700 °C expt, −
V_2O_5, −1552 VO_2, −714 V_2O_3, −1229 VO, −431	VCl_4, −570 VCl_3, −581 VCl_2, −460	−28/148.5	chloride formation, low; T > 100 °C; high vapor pressure expected, very low expt, very low; T > 200 °C[19,82]
ZnO, −349	$ZnCl_2$, −415 $ZnCl{\cdot}nH_2O$	290/732	chloride formation, high; T > 300 °C; high vapor pressure expected to be low expt, −
ZrO_2, −1089	$ZrCl_4$, −981 $ZrCl_3$, 710 $ZrCl_2$, −500 $ZrOCl_2{\cdot}8H2O$	330/437 −/− −/− 150 °C decomp	chloride formation, low; T > 400 °C; high vapor pressure expected to be medium; T < 500 °C expt, −

[a]These data are used to estimate the (expected) stability of Deacon catalysts. Where possible, the expected stability is compared with experiments (expt). The data are taken from Holleman and Wiberg[87] and from thermodynamic data available from Indiana University. http://courses.chem.indiana.edu/c360/documents/thermodynamicdata.pdf.

temperature, the lower the inherent stability of the catalyst. Therefore, active catalysts, which allow for lower reaction temperatures, are intrinsically more stable. For instance, RuO_2 is sufficiently active already around 550 K. If increasing the temperature to 650 K to increase activity, the stability of RuO_2 cannot be guaranteed. Rather, volatile Ru chlorides are formed, which leave the catalyst bed and sublime at the reactor outlet.[81] On the other hand, CuO-based catalysts are unstable above 400 °C under typical stoichiometric reaction mixtures. However, if one goes to reaction feeds with excess oxygen, then CuO-based catalysts are stable even at temperatures above 400 °C.[92,93]

Last but not least, the presented descriptor is important not only for ranking the experimentally observed activities of the catalysts in the Deacon process but, rather, may be equally important for oxidation catalysis by oxides catalysts in general.

AUTHOR INFORMATION

Corresponding Author

*(H.O.) Fax: ++49-641-9934559. E-mail: Herbert.Over@phys.chemie.uni-giessen.de. (R.S.) Fax: ++49-30-31479552. E-mail: schomaecker@tu-berlin.de.

Notes

The authors declare no competing financial interest.

ACKNOWLEDGMENTS

We would like to thank all our co-workers who have participated in this exciting project and whose names can be seen from the references. Franziska Hess and Philipp Krause are acknowledged for providing some of the figures presented in this Review. This Deacon project was supported by the federal ministry of science and education (BMBF_Deacon: 033R018C). The author appreciates intense discussions with partners of the BMBF project: Dr. T. Schmidt (Bayer Material Science), Dr. N. Lopez, Prof. J. Perez-Ramirez, Dr. D. Teschner, Prof. W. F. Maier, and Prof. K. Stöwe. Special thanks go to Dr. Felix Studt, Prof. B. Wang, and Dr. Alejandro Montoya, who provided us with values of oxygen dissociation energies.

REFERENCES

(1) Seki, K. *Catal. Surv. Asia* **2010**, *14*, 168.
(2) Perez-Ramirez, J.; Mondelli, C.; Schmidt, T.; Schlüter, O.F.-K.; Wolf, A.; Mleczko, L.; Dreier, T. *Energy Environ. Sci.* **2011**, *4*, 4786.
(3) Over, H. *J. Phys. Chem C* **2012**, *116*, 6779.
(4) Deacon, H. *U.S. Patent* 1656802, 1875.
(5) Johnson, A. J.; Cherniavsky, A. J. U.S. Patent 2542,961, 1951.
(6) Quant, J. T.; van Dam, J.; Engel, F.; Wattemena, F. *Chem. Eng.* **1963**, No. July/August, 224.
(7) Allen, J. A.; Clark, A. J. *Rev. Pure Appl. Chem.* **1971**, *21*, 145.
(8) Mitsui Toatsu Chemicals: A modern version of the Deacon process. *Chemical Week*, **1987**, June 24, 18.
(9) Mortensen, M.; Minet, R. G.; Tsotsis, T. T.; Benson, S. *Chem. Eng. Sci.* **1996**, *15*, 2031.
(10) Nieken, U.; Watzenberger, O. *Chem. Eng. Sci.* **1999**, *54*, 2619.
(11) Itoh, H.; Kono, Y.; Ajioka, M.; Takezaka, S.; Katzita, M. U.S. Patent 4803, 065, 1989
(12) Kiyoura, T.; Kogure, Y.; Nagayama, T.; Kanaya, K. U.S. Patent 4822,589, 1989.
(13) Yasuaki, T. *Stud. Surf. Sci. Catal.* **1995**, *92*, 41.
(14) Gestermann, F.; Ottaviani, A. *Modern Alkali Technology* **2001**, *8*, 49−56.
(15) Crihan, D.; Knapp, M.; Zweidinger, S.; Lundgren, E.; Weststrade, C. J.; Andersen, J. N.; Seitsonen, A. P.; Over, H. *Angew. Chem., Int. Ed.* **2008**, *47*, 2131.
(16) Zweidinger, S.; Hofmann, J. P.; Balmes, O.; Lundgren, E.; Over, H. *J. Catal.* **2010**, *272*, 169.
(17) Hofmann, J. P.; Zweidinger, S.; Knapp, M.; Seitsonen, A. P.; Schulte, K.; Andersen, J. N.; Lundgren, E.; Over, H. *J. Phys. Chem. C* **2010**, *114*, 10901.
(18) Hofmann, J. P.; Zweidinger, S.; Seitsonen, A. P.; Farkas, A.; Knapp, M.; Balmes, O.; Lundgren, E.; Andersen, J. N.; Over, H. *Phys. Chem. Chem. Phys.* **2010**, *12*, 15358.

(19) Hisham, M. W. M.; Benson, S. W. *J. Phys. Chem.* **1995**, *99*, 6194.
(20) Allen, J. A. *J. Appl. Chem (London)* **1962**, *12*, 406.
(21) Studt, F.; Abild-Pedersen, F.; Hansen, H. A.; Man, I. C.; Rossmeisl, J.; Bligaard, T. *ChemCatChem* **2010**, *2*, 98.
(22) Zweidinger, S.; Crihan, D.; Knapp, M.; Hofmann, J. P.; Seitsonen, A. P.; Lundgren, E.; Weststrate, C. J.; Andersen, J. N.; Over, H. *J. Phys. Chem. C* **2008**, *112*, 9966.
(23) Lopez, N.; Gomez-Segura, J.; Marin, R. P.; Perez-Ramirez, J. *J. Catal.* **2008**, *255*, 29.
(24) Teschner, D.; Farra, R.; Yao, L.; Schlogl, R.; Soerijanto, H.; Schomäcker, R.; Schmidt, T.; Szentmiklosi, L.; Amrute, A. P.; Modelli, C.; Perez-Ramirez, J.; Novell-Leruth, G.; Lopez, N. *J. Catal.* **2012**, *285*, 273.
(25) Toftelund, A.; Man, I. C.; Hansen, H. A.; Abild-Pedersen, F.; Bligarrd, T.; Rossmeisl, J.; Studt, F. *ChemCatChem* **2012**, *4*, 1856.
(26) Seitsonen, A. P.; Over, H. *J. Phys. Chem. C* **2010**, *114*, 22624.
(27) Kim, Y. D.; Seitsonen, A. P.; Wendt, S.; Wang, J.; Fan, C.; Jacobi, K.; Over, H.; Ertl, G. *J. Phys. Chem. B* **2001**, *105*, 3752.
(28) Wang, H.; Schneider, W. F.; Schmidt, D. *J. Phys. Chem. C* **2009**, *113*, 15266.
(29) Knapp, M.; Crihan, D.; Seitsonen, A. P.; Over, H. *J. Am. Chem. Soc.* **2005**, *127*, 3236.
(30) Hess, F.; Hofmann, J. P.; Seitsonen, A. P.; Over, H. *unpublished DFT calculations*; Aug. 2011.
(31) Hess, F.; Krause, P. P. T.; Rohrlack, S. F.; Hofmann, J. P.; Farkas, A.; Over, H. *Surf. Sci. Surf. Sci. Lett.* **2012**, *606*, L69.
(32) Hong, S.; Karim, A.; Rahman, T. S.; Jacobi, K.; Ertl, G. *J. Catal.* **2010**, *276*, 371.
(33) Schneider, W. F. *Surf. Sci.* **2012**, *606*, 1351.
(34) Bronsted, J. N. *Chem. Rev.* **1928**, *5*, 231.
(35) Evans, M. G.; Polanyi, M. *Trans. Faraday Soc.* **1938**, *34*, 11.
(36) Pallassana, V.; Neurock, M. *J. Catal.* **2000**, *191*, 301.
(37) Norskov, J. K.; Bligaard, T.; Logadottir, A.; Bahn, S.; Hansen, L. B.; Bollinger, M.; Bengaard, H.; Hammer, B.; Sljivancanin, Z.; Mavrikakis, M.; Xu, Y.; Dahl, S.; Jacobsen, C. J. H. *J. Catal.* **2002**, *209*, 275.
(38) Liu, E.-P.; Hu, P. *J. Chem. Phys.* **2001**, *114*, 8244.
(39) Michaelidides, A.; Liu, Z.-P.; Zhang, C. J.; Alavi, A.; King, D. A.; Hu, P. *J. Am. Chem. Soc.* **2003**, *125*, 3704.
(40) Logadottir, A.; Rod, T. H.; Norskov, J. K.; Hammer, B.; Dahl, S.; Jacobsen, C. J. H. *J. Catal.* **2001**, *197*, 229.
(41) Crawford, P.; McAllister, B.; Hu, P. *J. Phys. Chem. C* **2009**, *113*, 5222.
(42) Vojvodic, A.; Calle-Vallejo, F.; Guo, W.; Wang, S.; Toftelund, A.; Studt, F.; Martinez, J. I.; Shen, J.; Man, I. C.; Rossmeisl, J.; Bligaard, T.; Norskov, J. K.; Abild-Pedersen, F. *J. Chem. Phys.* **2011**, *134*, 244509.
(43) Allen, J. A.; Clark, A. J. *Rev. Pure Appl. Chem.* **1971**, *21*, 145.
(44) Mortensen, M.; Minet, R. G.; Tsotsis, T. T.; Benson, S. W. *Chem. Eng. Sci.* **1999**, *54*, 2131.
(45) Nieken, U.; Watzenberger, O. *Chem. Eng. Sci.* **1999**, *54*, 2619.
(46) Over, H. *Electrochim. Acta* **2013**, *93*, 314.
(47) Trasatti, S. *Electrochim. Acta* **2000**, *45*, 2377.
(48) Amrute, A. P.; Mondelli, C.; Moser, M.; Novell-Leruth, G.; Lopez, N.; Rosenthal, D.; Farra, R.; Schuster, M. E.; Schuster, D.; Schmidt, T.; Perez-Ramirez, J. *J. Catal.* **2012**, *286*, 287.
(49) Suleiman, I. A.; Mackie, J. C.; Kennedy, E. M.; Radny, M. W.; Dlugogorski, B. Z. *Chem. Phys. Lett.* **2011**, *501*, 215.
(50) Rozanska, X.; Sauer, J. *Int. J. Quantum Chem.* **2008**, *108*, 2223.
(51) Boreskov, G. K. *Adv. Catal.* **1965**, *15*, 285.
(52) Hutchings, G. J.; Taylor, S. H. *Catal. Today* **1999**, *49*, 105.
(53) Amrute, A. P.; Mondelli, C.; Hevia, M. A. G.; Perez-Ramirez, J. *J. Phys. Chem. C* **2011**, *115*, 1056.
(54) Amrute, A. P.; Modelli, C.; Perez-Ramirez, J. *Catal. Sci. Technol.* **2012**, *2*, 2057.
(55) Ruetschi, P.; Delahay, P. *J. Chem. Phys.* **1955**, *23*, 556.
(56) Klissurs, D.; Dikova, R. P. *Z. Phys. Chem. (Leipzig)* **1969**, *241*, 101.
(57) Trasatti, S. *J. Electroanal. Chem.* **1980**, *111*, 125.
(58) Trasatti, S. *Electrochim. Acta* **1984**, *29*, 1503.
(59) Trasatti, S.; O'Grady, W. E. In *Advances in Electrochemistry and Electrochemical Engineering*; Gericher, H., Tobias, C. W., Eds.; Wiley: New York, 1980; Vol *13*, p 177.
(60) Soerijanto, H.; Schomaecker, R.; Schmidt, T. *Unpublished activity screening experiments*; 2012.
(61) Hansen, H. A.; Man, I. C.; Studt, F.; Abild-Pedersen, F.; Bligaard, T.; Rossmeisl, J. *J. Phys. Chem. Chem. Phys.* **2010**, *12*, 283.
(62) Rossmeisl, J.; Qu, Z.-W.; Zhu, H.; Kroes, G.-J.; Norskov, J. K. *J. Electroanal. Chem.* **2007**, *607*, 83.
(63) Norskov, J. K.; Bligaard, T.; Rossmeisl, J.; Christensen, C. H. *Nat. Chem.* **2009**, *1*, 37.
(64) Norskov, J. K.; Abild-Pedersen, F.; Studt, F.; Bligaard, T. *Proc. Natl. Acad. Sci. U.S.A.* **2011**, *108*, 939.
(65) Over, H. *Chem. Rev.* **2012**, *112*, 3356.
(66) Wang, C. C.; Siao, S. S.; Jiang, J. C. *J. Phys. Chem. C* **2011**, *116*, 6367.
(67) Wendt, S.; Schaub, R.; Matthiesen, J.; Vestergaard, E. K.; Wahlström, E.; Rasmussen, M. D.; Thostrup, P.; Molina, L. M.; Lægsgaard, E.; Stensgaard, I.; Hammer, B.; Besenbacher, F. *Surf. Sci.* **2005**, *598*, 226.
(68) Man, I. C.; Su, H.-Y.; Calle-Vallejo, F.; Hansen, H. A.; Martinez, J. I.; Inoglu, N. G.; Kitchin, J.; Jaramillo, T. F.; Norskov, J. K.; Rossmeisl, J. *ChemCatChem* **2011**, *3*, 1159.
(69) The linear relation is $\Delta E_{diss} = 2 \times (\Delta E_{O^*} - 2.6)$ in eV.
(70) Amrute, A. P.; Mondelli, C.; Hevia, M. A. G.; Perez-Ramirez, J. *ACS Catal.* **2011**, *1*, 583.
(71) Montoya, A.; Haynes, B. S. *Chem. Phys. Lett.* **2011**, *502*, 63.
(72) Shojaee, K.; Montoya, A.; Haynes B. S.; *unpublished calculations*; Oct. 2012.
(73) Zhang, R.; Liu, H.; Wang, B.; Ren, J.; Li, Z. *Appl. Surf. Sci.* **2011**, *258*, 408.
(74) Zhang, R.; Liu, H.; Zheng, H.; King, L.; Li, Z.; Wang, B. *Appl. Surf. Sci.* **2011**, *257*, 4787.
(75) Mondelli, C.; Amrute, A. P.; Schmidt, T.; Perez-Ramirez, J. *Chem. Commun.* **2011**, *47*, 7173.
(76) Palmer, M. S.; Neurock, M.; Olken, M. M. *J. Phys. Chem B* **2002**, *106*, 6543.
(77) Seitsonen, A. P.; Over, H. *Surf. Sci.* **2009**, *603*, 1717.
(78) Reuter, K.; Scheffler, M. *Phys. Rev. B* **2001**, *65*, 035406.
(79) Hevia, M. A.; Amrute, A. P.; Schmidt, T.; Perez-Ramirez, J. *J. Catal.* **2010**, *276*, 141.
(80) Mondelli, C.; Amrute, A. P.; Krumreich, F.; Schmidt, T.; Perez-Ramirez, J. *ChemCatChem* **2011**, *3*, 657.
(81) Kanzler, C., Urban, S.; Hess, F.; Zalewska-Wierzbicka, K.; Rohrlack, S. F.; Wessel, C.; Ostermann, R.; Hofmann, J.-P.; Samrsly, B.; Over, H. Unpublished; 2012.
(82) Tarabanko, V. E.; Tarabanko, N. V.; Koropachinskaya, N. V. *Catal. Ind.* **2010**, *2*, 259.
(83) Tarabanko, V. E.; Tarabanko, N. V.; Zhyzhaev, A. M.; Koropachinskaya, N. V. *J. Sib. Fed. Univ. Chem.* **2009**, *1*, 11.
(84) Ganduglia-Piovano, M. V.; Sauer, J. *Phys. Rev. B* **2004**, *70*, 045422.
(85) Soon, A.; Todorova, M.; Delley, B.; Stampfl, C. *Surf. Sci.* **2007**, *601*, 5809.
(86) Soon, A.; Todorova, M.; Delley, B.; Stampfl, C. *Phys. Rev. B* **2007**, *75*, 125420.
(87) Holleman, A. F.; Wiberg, E. *Lehrbuch der Anorganischen Chemie*; Walter de Gryter: Berlin, 1995.
(88) Hagemeyer, A.; Trübenbach, P.; Rieker, C. W.; Watzenberger, O.; EP Patent 0761594-A1, assigned to BASF AG, 1997.
(89) Mondelli, C.; Amrute, A. P.; Moser, M.; Novell-Leruth, G.; Lopez, N.; Rosenthal, D.; Farra, R.; Schuster, M. E.; Teschner, D.; Schmidt, T.; Perez-Ramirez, J. *J. Catal.* **2012**, *286*, 287.
(90) Pan, H. Y.; Minet, R. G.; Benson, S. W.; Tsotsis, T. T. *Ind. Eng. Chem. Rev.* **1994**, *33*, 2996.
(91) Honkala, K.; Hellman, A.; Remediakis, I. N.; Logadottir, A.; Carlsson, A.; Dahl, S.; Christensen, C. H.; Norskov, J. K. *Science* **2005**, *307*, 5709.

(92) Schomäcker, R., Maier, W. F. *Private communication*; August 2012.
(93) Hammes, M.; Valtchev, M.; Roth, M. B.; Stöwe, K.; Maier, W. F. *Appl. Catal., B* **2013**, *132−133*, 389.